

Liverpool Preprint: LTH 346
 TFT Preprint: HU-TFT-95-21
 hep-lat/9503018
 14th March, 1995

Cooling and the $SU(2)$ instanton vacuum

C. Michael

DAMTP, University of Liverpool, UK

P.S. Spencer

TFT, University of Helsinki, Finland

Abstract

We present results of an investigation into the nature of instantons in 4-dimensional pure gauge lattice $SU(2)$ obtained from configurations which have been cooled using an under-relaxed cooling algorithm. We discuss ways of calibrating the cooling and the effects of different degrees of cooling, and compare our data for the shapes, sizes and locations of instantons with continuum results. In this paper we extend the ideas and techniques developed by us for use in $O(3)$, and compare the results with those obtained by other groups.

1 Introduction

Much work has been done in simulating the $SU(2)$ vacuum, with the aim of learning more about the vacuum structure of QCD, and a lot of interest has been shown in the existence of instantons in this vacuum. Early studies into the cooled $SU(2)$ vacuum were carried out in [1], where, working on a lattice with ‘zero-derivative’ boundary conditions rather than the more usual periodic boundaries, Teper investigated the role of instantons by locally minimizing the action (ie. cooling) and concluded that the lattice $SU(2)$ theory does indeed contain instantons, but that the large, physically important ones will be absent in studies with $\beta \leq 2.7$. At the same time, in [2], Ilgenfritz *et al*, working on 6^4 lattices at $\beta = 2.1, 2.2$, found (multi-)instanton solutions from successive coolings of the (equilibrated) gauge fields:

$$U_{x,\mu} \rightarrow U'_{x,\mu} = c\Sigma_{x,\mu} \quad (1)$$

where c is a normalisation constant to ensure $U'_{x,\mu} \in SU(2)$ and Σ is the sum of six staples (this will be equivalent to taking $\alpha = 0$ in eq. 21). They found that

the action density is concentrated in distinct, separated parts of the lattice — consistent with the picture of a dilute instanton gas — and that these lattice instantons are meta-stable under cooling of the gauge fields, being shrunk in size and finally annihilated by prolonged cooling. They also studied the eigenvalue spectra of the fermion zero modes, and concluded that $SU(2)$ on the lattice does indeed have an instanton vacuum.

In [3], Polikarpov and Veselov, working on 8^4 – 12^4 lattices at $\beta = 2.3, 2.35$ carried out a detailed study of the cooling process and identified five distinct stages in the history of a cooled configuration: (i) freezing of quantum fluctuations and the arising of quasi-classical configurations of instanton–anti-instanton type; (ii) smoothing of quantum fluctuations around instantons and anti-instantons; (iii) annihilation of instantons and anti-instantons; (iv) a long stage involving the existence of classical solutions; (v) a short stage involving the disappearance of classical solutions.

The classification of these stages is, in their own words, somewhat arbitrary, with an absence of definite borders between the stages. They found that there were (at least) two characteristic points on the cooling curve, however: around the middle of stage (iv) they found a zero of $\Delta^2 S(N)$ (corresponding to the second derivative of S with respect to cooling sweep N), and another somewhere on the border between stages (ii) and (iii) at which $\Delta^2 S(N) \approx 0$. They calibrated their cooling process by stopping at the former point; they denoted a configuration in this state as an ‘instanton vacuum’, and identified the latter point as the beginning of the instanton–anti-instanton annihilation, denoted as the ‘instanton–anti-instanton vacuum’.

This paper is organised as follows: in section 2 we outline the formalism of continuum $SU(2)$, and briefly discuss the instanton solution found by Belavin *et al* in [4]; in section 3 we consider how to construct an $SU(2)$ instanton on a periodic lattice; in section 4 we discuss calibrating the cooling we use, with a first calibration attempt given in subsection 4.1 and a better method given in subsection 4.2; in section 5 we detail the means of locating and sizing the instantons, compare their shapes with the form of isolated, continuum objects and calculate a size distribution for them; in section 6 we consider inter-instanton separations and compare our results with refs. [5, 6]. Our conclusions are given in section 7. The figures referred to in the text are collected together at the end of the paper. Preliminary results from this work were presented at Lattice 94 [7].

2 Instantons in $SU(2)$

As in 2-dimensional $O(3)$, 4-dimensional $SU(2)$ has instanton solutions¹ due, in this case, to the homotopy class of mappings from $S_3 \rightarrow S_3$, ie from the points

¹This section follows the discussion of Yang-Mills instantons given in [8].

on a four-dimensional sphere parameterised by three angles, to the elements of $SU(2)$, which is also determined by three parameters. In other words, the $SU(2)$ group manifold is topologically equivalent to S_3 : any $SU(2)$ group element can be written in terms of the Pauli matrices as

$$U = u_4 \mathbf{1} + i \mathbf{u} \cdot \boldsymbol{\sigma} \quad ; \quad u_4^2 + \mathbf{u}^2 = 1 \quad , \quad \boldsymbol{\sigma} = (\sigma_1, \sigma_2, \sigma_3) \quad (2)$$

with $\mathbf{1}$ the 2×2 unit matrix, and $u = (u_4, \mathbf{u})$ clearly defining a point on S_3 , the sphere in 4-dimensional Euclidean space. Mappings in this case are characterised by the topological charge Q^T defined in terms of the divergence of a (gauge-dependent) current:

$$Q^T = \frac{1}{16\pi^2} \int d^4x \operatorname{tr} F_{\mu\nu} \tilde{F}_{\mu\nu} \quad (3)$$

$$\partial_\mu K_\mu = 2 \operatorname{tr} (F_{\mu\nu} \tilde{F}_{\mu\nu}) \quad (4)$$

$$K_\alpha = 4 \varepsilon_{\alpha\beta\gamma\delta} \operatorname{tr} (A_\beta \partial_\gamma A_\delta + \frac{2}{3} A_\beta A_\gamma A_\delta) \quad (5)$$

with the gauge fields and field strength tensor scaled by i/g and defined by

$$F_{\mu\nu} = \partial_\mu A_\nu - \partial_\nu A_\mu + [A_\mu, A_\nu] \quad (6)$$

and the dual of F given by $\tilde{F}_{\mu\nu} = \frac{1}{2} \varepsilon_{\mu\nu\lambda\rho} F_{\lambda\rho}$. Under a gauge transformation $T(x_\mu)$ we have

$$A_\mu \rightarrow T^\dagger A_\mu T + T^\dagger \partial_\mu T \quad (7)$$

To find the instanton solutions we look for finite-action solutions to classical Euclidean Yang-Mills theory. In order to have the action

$$S = \frac{1}{2g^2} \int d^4x \operatorname{tr} F_{\mu\nu} F_{\mu\nu} \quad (8)$$

finite we require $F_{\mu\nu}(x) \xrightarrow{|x| \rightarrow \infty} 0$ which we can take to mean $A_\mu(x) \xrightarrow{|x| \rightarrow \infty} 0$. However, in practice this is too restrictive, and eq. 7 means we only need

$$A_\mu(x) \rightarrow T^\dagger \partial_\mu T \text{ as } |x| \rightarrow \infty \quad (9)$$

which is obtained from $A_\mu = 0$ by a gauge transformation. To find the fields satisfying this boundary condition we make use of the following positivity relation

$$\operatorname{tr} \int d^4x (F_{\mu\nu} \pm \tilde{F}_{\mu\nu})^2 \geq 0 \quad (10)$$

As

$$(F_{\mu\nu} \pm \tilde{F}_{\mu\nu})^2 = 2(F_{\mu\nu} F_{\mu\nu} \pm F_{\mu\nu} \tilde{F}_{\mu\nu}) \quad (11)$$

we have

$$\operatorname{tr} \int d^4x F_{\mu\nu} F_{\mu\nu} \geq \left| \operatorname{tr} \int d^4x F_{\mu\nu} \tilde{F}_{\mu\nu} \right| = 16\pi^2 Q \quad (12)$$

using the definition for Q given in eq. 3. From this we have

$$S \geq \frac{8\pi^2}{g^2}Q \quad (13)$$

whence we see that the action for a single instanton is $S_I = 8\pi^2/g^2$ (cf. the result for $O(3)$: $S_I = 4\pi/g^2$). Clearly, then, the action is minimised for the (anti-)self dual solutions $F_{\mu\nu} = \pm\tilde{F}_{\mu\nu}$.

In looking for the instanton solution, Belavin *et al* [4] considered first $O(4)$ gauge theory, isomorphic to $SU(2) \times SU(2)$ with one $SU(2)$ identified with the internal symmetry and the other with the three-sphere at $|x| \rightarrow \infty$. The resulting gauge transformation has the form

$$T(x) = \frac{1}{|x|}(x_4 + i\mathbf{x} \cdot \boldsymbol{\sigma}) \text{ with } |x|^2 = x_4^2 + \mathbf{x}^2 \quad (14)$$

giving rise to a gauge field

$$A_\mu(x) = \frac{x^2}{\rho^2 + x^2}T^\dagger(x)\partial_\mu T(x) \quad (15)$$

where ρ is the instanton size, and $x = 0$ its centre. For $x^2 \gg \rho^2$, $A_\mu \rightarrow T^\dagger\partial_\mu T$ as required by eq. 9. We can write the space and time components of A_μ explicitly as

$$A_4(x) = \frac{-i\mathbf{x} \cdot \boldsymbol{\sigma}}{x^2 + \rho^2} \quad (16)$$

$$\mathbf{A}(x) = \frac{i(x_4\boldsymbol{\sigma} + \boldsymbol{\sigma} \times \mathbf{x})}{x^2 + \rho^2}. \quad (17)$$

2.1 Instanton–anti-instanton interactions

Thus far we have only considered the single-instanton solution; multi-instanton configurations can be generated by simply multiplying instanton fields with their centres at different locations [9], and calculations involving mixed instanton–anti-instanton configurations are non-trivial. In [5], Förster considered an instanton–anti-instanton pair at large separation, taking an instanton at $x = 0$, given by eq. 15, and an anti-instanton at $x = C$, given by:

$$A'_\mu(x) = \frac{(x - C)^2}{\lambda^2 + (x - C)^2}T(x - C)\partial_\mu T^\dagger(x - C) \quad (18)$$

with λ the size parameter for the anti-instanton. By performing a conformal mapping, the point $x = C$ is sent to infinity and the local behaviour at $x = C$

implies the interaction takes the form of a kink and an anti-kink separated by a distance $-\log(\rho\lambda)$ giving an interaction term:

$$S_{\text{int}} = -48 \frac{\pi^2}{g^2} \frac{\rho^2 \lambda^2}{(x_1 - x_2)^4} \quad (19)$$

with g^2 the coupling occurring in eq. 8 above, implying an attraction between unlike objects. In [6], Palmer and Pinsky, investigating this interaction and the distinction between dilute and dense phases of the instanton gas, considered the case of an instanton–anti-instanton pair separated by the size of one member, with the size of the other free. They found that there was a minimum finite separation:

$$c = \rho = 2\lambda \quad (20)$$

at which point the pair melts into a pure gauge with zero action. This will be relevant when we investigate the separations of objects in section 6 below.

3 $SU(2)$ instantons on the lattice

We seek to extend the successful calibrated cooling method [10, 11] from $O(3)$ to $SU(2)$. As before, we use an under-relaxed cool, in this case given by

$$U'_{x,\mu} = \Sigma_{x,\mu} + \alpha U_{x,\mu} \quad (21)$$

where $\Sigma_{x,\mu}$ is the sum of the six ‘staples’ around the link $U_{x,\mu}$, and $U'_{x,\mu}$ is subsequently normalised to lie in $SU(2)$. Following the results of [10, 11] we take $\alpha = 2$.

In order to calibrate the cooling, we want to generate a gauge configuration by using a suitable lattice version of eq. 15, as we intend to calibrate the cooling by examining its effects on a particular known configuration. However, this formula is explicitly incompatible with periodic boundary conditions¹, as we require the A_μ fields to vanish at large distances from the instanton centre². In order to achieve this we must construct the instanton as follows [12]: first construct the $A_\mu(x)$ in R^4 as above. Next construct the link variables $U_{x,\mu}$ from these continuum fields. As stated above, we require an instanton solution to be self-dual, and for the lattice solution this relation is only approximate. If we take as the link fields

$$U_{x,\mu} = \exp(i[A_\mu(x) + A_\mu(x + \mu)]/2) \quad (22)$$

constructing these on an infinite lattice, then the deviation from self-duality is $\mathcal{O}(\rho^{-2})$ [12]. Next we perform a singular gauge transformation *on the lattice*

¹We are greatly indebted to Mike Teper for discussion on this subject.

²The concept of “large distance” on a periodic lattice may seem a strange one. What we need, for a moderately sized instanton sited at the centre of the lattice, is that the A_μ fields approach zero at the lattice boundary.

using eq. 14, with the singularity ‘off-site’ both here and in the construction of the $A_{x,\mu}$ fields:

$$U_{x,\mu} = T_x U_{x,\mu} T_{x+\mu}^\dagger \quad (23)$$

(where T_x denotes the gauge transformation on the site x of the infinite lattice) and finally we impose periodicity on the solution by enforcing

$$U_\mu(x_i = -L/2) \equiv U_\mu(x_i = +L/2) \quad (24)$$

for each x_i and each μ for a L^4 lattice.

In constructing this solution we must also take into account the fact that eq. 15 gives the instanton in terms of the $A_\mu(x)$ fields, while on the lattice we need to use the $U_{x,\mu}$ link fields, and so need to rewrite the instanton solution in terms of these link variables. This is straightforward as

$$\exp(i\theta \hat{\mathbf{x}} \cdot \boldsymbol{\sigma}) = \cos \theta + i(\hat{\mathbf{x}} \cdot \boldsymbol{\sigma}) \sin \theta \quad (25)$$

and we can rewrite eq. 15 in this form. The individual components are, explicitly:

$$iA_4(x) = \frac{1}{x^2 + \rho^2} (\boldsymbol{\sigma} \cdot (x_1, x_2, x_3)) \quad (26)$$

$$iA_1(x) = \frac{-1}{x^2 + \rho^2} (\boldsymbol{\sigma} \cdot (x_4, x_3, -x_2)) \quad (27)$$

$$iA_2(x) = \frac{-1}{x^2 + \rho^2} (\mathbf{sigma} \cdot (-x_3, x_4, x_1)) \quad (28)$$

$$iA_3(x) = \frac{-1}{x^2 + \rho^2} (\mathbf{sigma} \cdot (x_2, -x_1, x_4)) . \quad (29)$$

As in $O(3)$, this field configuration is metastable (with the Wilson gauge action we are using) and will be annihilated by prolonged cooling. (See the discussion in [10, 11]). For instantons where ρ is not small compared to L there will be significant discontinuities across the lattice boundary, which can be removed by a moderate amount of cooling.

4 Calibrating the under-relaxed cooling.

We performed our simulations on a CRAY Y-MP, using 16^4 and 24^4 lattices at $\beta = 2.4, 2.5$ respectively. These correspond to lattice spacings of approximately 0.12fm and 0.08fm [13]. Each of our configurations is generated from 500 updates with 1 heatbath update followed by 3 over-relaxation updates, after several thousand thermalisation sweeps. In fig. 1 we present the cooling history of two example $SU(2)$ gauge configurations, calculated on the smaller lattice.

4.1 A first attempt at calibration

For $O(3)$, we concluded [11] that an optimum cooling would be that required to annihilate an instanton of size $\rho = \mathcal{O}(2a)$ where a is the lattice spacing. In table 1 there is shown the number of cooling sweeps at $\alpha = 2$ (which we had decided was a good compromise between cooling too severely and making too many cooling sweeps) needed to remove $SU(2)$ instantons of size $\rho = a, 3a/2, 2a, 4a$ generated from the prescription above. It transpires that these are much more stable under cooling than their $O(3)$ counterparts.

ρ	a	$3a/2$	$2a$	$4a$
N_{sweeps}	495	503	510	536

Table 1: The number of sweeps N_{sweeps} at $\alpha = 2$ required to annihilate (to reduce S/S_I to < 0.1) a single $SU(2)$ instanton of size ρ . Calculated on a 16^4 lattice at $\beta = 2.4$, with the instanton positioned off-site in the centre of the lattice.

This much greater stability presents us with something of a dilemma: were we to naïvely proceed and take the value for $\rho = 2a$ in table 1 as a calibrator, then the gauge configurations we would have after cooling would be well past the first three stages defined by Polikarpov and Veselov above — which is where we wish to examine the vacuum, as we wish to study its structure in the presence of (anti-)instantons — and in some cases will have been cooled so far as to entirely remove all vacuum structure. There are two possible candidates from the cooling curve of annihilation of a single instanton for the level of cooling to use. The first is the cooling required to remove the undesired boundary effects, while the second is the amount required to then annihilate the instanton, once the boundary discontinuities have been eliminated. However, neither of these methods of calibration is really satisfactory — the former is too unphysical a process, as it removes what is essentially a lattice artefact that has nothing to do with the underlying physics, and given the size of the lattice and the value of β we use, the latter seems excessive when compared to the results presented in [11]. In light of this we propose a different means of calibration.

4.2 A second calibration method

As we wish to model the vacuum as quantum fluctuations around classical configurations, we first generate a classical configuration: the single-instanton solution as presented above. We then cool this by enough sweeps to remove any boundary discontinuities. Next we perform a few heatbath updates at the β value under study to introduce some quantum fluctuations and then cool it until we regain the original configuration, ie until $S = S_I \pm 10\%$.

Quite how many heatbath sweeps to perform is open to question: we seek to reach a state in some respects similar to the uncooled configurations, but not too far away from the original instanton — we do not want to introduce any more structure than was already present. We found that, at $\beta = 2.4$ on a 16^4 lattice, 10 heatbath sweeps was optimum for introducing the required quantum fluctuations without overly changing the underlying structure, whereas for $\beta = 2.5$ on a 24^4 lattice, 10 was too few and, at this higher β value, we found 20 were required. As a check of this we found 20 too many for the lower β on the larger lattice, with new structure occurring in more than half of the sample configurations we looked at; by comparison, for $\beta = 2.5$, 20 sweeps introduced new structure¹ in less than 5% of the ensemble.

As a further check of the validity of the number of thermalisation sweeps used, we looked at the value of $\langle \text{tr}U_{\square} \rangle$ on the configuration. We found that with 10 heating sweeps on the $\beta = 2.4$, 16^4 lattice this was consistent with established results, and this was also true for 20 sweeps on the $\beta = 2.5$, 24^4 configurations, while half the number of sweeps in each case gave a value that was too high. These two checks — not introducing more structure, and heating until the correct value of $\langle \text{tr}U_{\square} \rangle$ is attained at a given β value — form respectively effective upper and lower bounds on the number of heatbath sweeps to be performed.

The calibration results are given in table 2 for initial configurations each containing a single instanton of size $\rho = a, 2a, 3a, 4a$.

In [11] we decided that a good check on whether the cooling had taken the configuration to the same physical state was whether or not there was a good agreement across β of the value of $\langle S/V_{\text{phys}}S_I \rangle$, and found that the criteria we used for $O(3)$ led to such an agreement. For our $SU(2)$ data however, the agreement appears to be less good, with $\langle S/V_{\text{phys}}S_I \rangle = 0.000185(2)$ at $\beta = 2.4$ and $\langle S/V_{\text{phys}}S_I \rangle = 0.000249(3)$ at $\beta = 2.5$. While not equal, these two numbers seemed sufficiently close for us to accept this calibration method, although no doubt these values could be brought closer by a certain amount of ‘fine-tuning’. On the basis of these results we chose 72 sweeps to be the number required at $\beta = 2.4$ with $\alpha = 2$, and 154 sweeps at $\beta = 2.5$, and accepted this method as a calibration technique for under-relaxed cooling in $4d$ $SU(2)$.

5 Instanton size, shape and distributions

In [11] we found we could obtain good results for the sizes and locations of instantons using $S(x)$, although in principle $Q(x)$ contains more information. This was because in investigating the size distribution we were not concerned with

¹We ascertained whether the configuration had been moved away from the single-instanton solution by following the cooling history. Where new structure had been introduced by the heatbath sweeps, ‘steps’ appeared in the history, in much the same way as they appear in the solid line in fig. 1.

β	L	N_{heat}	ρ	N_{cool}	$\langle \text{tr}U_{\square} \rangle$
2.4	16	10	a	71(8)	0.6344(6)
			$2a$	72(7)	0.6346(5)
			$3a$	71(7)	0.6347(7)
			$4a$	73(5)	0.6345(5)
2.5	24	20	a	152(12)	0.6529(3)
			$2a$	155(8)	0.6530(3)
			$3a$	154(11)	0.6530(3)
			$4a$	154(13)	0.6530(3)

Table 2: The number of sweeps N_{cool} at $\alpha = 2$ required to restore a configuration with a single lattice instanton of size ρ after N_{heat} heatbath updates, and the value of the average plaquette after the heatbath sweeps. The figures in parentheses are one standard deviation, the data are obtained from 50 configurations in each case. The accepted values of $\langle \text{tr}U_{\square} \rangle$ are 0.63058(2)[$\beta = 2.4$] and 0.65235(1)[$\beta = 2.5$] [14].

the sign of the object. When we came to look at the inter-instanton separations, we still used $S(x)$ for calculating the locations and obtained information on the sign from $Q(x)$.

For $SU(2)$, we used the ‘plaquette’ method [15] to calculate $Q(x)$ on our cooled configurations:

$$Q_L(x) = \frac{1}{64\pi^2} (\text{tr} (\Pi_{x,12}\Pi_{x,34}) + \text{tr} (\Pi_{x,13}\Pi_{x,42}) + \text{tr} (\Pi_{x,14}\Pi_{x,23})) \quad (30)$$

where $\Pi_{x,ij}$ is the orientated path combination at x in the ij plane, consisting of the sum of the four clover leaves of $(U_{\square} - U_{\square}^{\dagger})/2$.

We choose the most local and symmetric definition for the action density at a site. We used the average of contributions from all plaquettes with one corner on the site x . This results in an action density that matches $Q(x)$ very well (and in the continuum $S(x) \propto Q(x)$ around an isolated instanton), but is not as smooth as $Q(x)$, as can be seen from figs. 2 and 3. Since $S(x)$ not as smooth as $Q(x)$, on occasion the instanton location algorithm will record more structure in a given area of the lattice than is actually there and will ignore valid structure elsewhere when applied to $S(x)$. For this reason we conducted our instanton search at $\beta = 2.4$ using both $S(x)$ and $Q(x)$.

Here we look at connected 4-dimensional regions of the lattice. We use the same method as in [11] by looking for local maxima in the density, and in this case use as a size parameter, which we denote ρ_L , the 4th root of the hypervolume of the connected region of sites for which the density is not less than half that

at the peak. In order to relate this ρ_L back to the size parameter in eq. 15, we define an effective radius (see ref. [16] for a similar prescription) ρ_{eff} :

$$\rho_{\text{eff}}^2 = \frac{\sqrt{2}}{\pi(\sqrt[4]{2}-1)} \rho_L^2. \quad (31)$$

This is the parameter plotted in figs. 4–7 and quoted in table 3. Eq. 13 gives a lower bound on the action, and so S/S_I can be interpreted as an upper bound on the number of objects in a given configuration, and we used this to determine how many we looked for in each configuration.

To see how closely the individual objects resemble isolated continuum instantons, we looked at the relation between the height at the peak and the calculated size, as these have the continuum relations

$$S_{\text{max}} = \frac{48}{g^2} \frac{1}{\rho^4} \quad (32)$$

and

$$Q_{\text{max}} = \frac{2g^2}{16\pi^2} S_{\text{max}} = \frac{6}{\pi^2 \rho^4} \quad (33)$$

for an isolated instanton. Our results are presented in figs. 4 and 5. All distances are in units of the lightest glueball mass, $\xi = 1/m_{0^+}$ with $m_{0^+}(2.4) = 0.94(8)$ and $m_{0^+}(2.5) = 0.63(8)$, taking the values for the lattice spacing a at these values of β from [13] and the mass of the 0^+ glueball at $\beta = 2.4$ from [17]. The data was obtained from 261 configs at $\beta = 2.4$ and 250 at $\beta = 2.5$.

As in [11] we calculated the distribution of instanton sizes. The data for $dN/Vd\rho$ are presented in figs. 6–7. All sizes are again in units of the correlation length, ξ . (It should be noted that the plot we presented earlier in [7] used ρ_L , scaled by a different factor from that above, rather than ρ_{eff} and so contained a peak in a different position.)

In agreement with [2, 3, 18] we find a distribution that grows with instanton size (unlike that presented for $O(3)$ in [11]), although our distribution lacks the sharp large-size cutoff they find; we attribute this to our means of determining the size from connected hyper-volumes whereas in [2, 3] they simply measured the size along the lattice axes. In [18], Chu *et al* measured the size by using the correlation function

$$f(x) = \sum_y Q(y)Q(x+y) \quad (34)$$

and comparing this with a convolution of the analytic expression:

$$Q_\rho(x) = \frac{6}{\pi^2 \rho^4} \left(\frac{\rho^2}{x^2 + \rho^2} \right)^4 \quad (35)$$

which they fitted to the lattice data for $f(x)$, obtained by cooling for 25 and 50 sweeps, using a single value of ρ they took to be an average size. Their

distribution was obtained, like ours, by analysing connected regions of the lattice, and extracting the size from the size of the region, their criterion being that two adjacent points belong to the same cluster if the product of $Q(x)$ at these points is greater than the square of some threshold parameter introduced because of the algebraic fall-off of the instanton. However, their methods and results rely heavily on the assumptions that the instantons are dilute — an assumption which we can see from figs. 2 and 3 is an unreliable one, particularly at their smaller degree of cooling.

Our distributions are peaked at around $3/m_{0+}$ at $\beta = 2.4$, and at $2/m_{0+}$ at $\beta = 2.5$. As in [9, 18] we find the smaller scale instantons, those with $\rho_L \leq 2a$, absent after cooling. Thus at smaller lattice spacing, we are able to explore the distribution down to smaller instanton sizes without distortion.

Results presented recently [19] showed a plateau in the distribution of sizes calculated on a lattice with twisted boundary conditions; our data, calculated using periodic boundary conditions, show no evidence of such a plateau.

Analagous to the discussion in [11], we can deduce a size distribution of the $SU(2)$ vacuum instantons in the dilute instanton gas approximation. In this case the distribution is expected to be [20]

$$\frac{1}{VS_I} \frac{dS}{d\rho} \sim \rho^{7/3} \quad (36)$$

Clearly our distributions do not display this behaviour. It should be noted that in this case the dilute instanton gas model gives a size distribution that is infra-red divergent, unlike the ultra-violet divergence for $O(3)$.

6 Instanton–anti-instanton separations

As before, in [11], we examined the separations of pairs of like and unlike objects (I-I, A-A and I-A pairs). There we found that the average closest separation of unlike pairs was significantly smaller, with the I-A pairs having a closest separation approximately 70–75% that of the I-I or A-A separations. In section 2.1 above, we showed how the interaction between unlike pairs is attractive and so isolated I-A pairs should be found to occur closer on average than I-I or A-A, but that I-A pairs closer than a certain minimum distance, given in eq. 20, mutually annihilate, so that we should not expect to find I-A pairs at smaller separations than when one is located on the boundary of the other with their sizes such that $R_{\min} = \rho_1 = 2\rho_2$. While we did not expect to find this relation exactly reproduced by the lattice results, as the instantons are not hyper-spherical and each pair will be influenced by every other object in the configuration to a greater or lesser degree, we were surprised to find that it is partially reproduced: the closest separation of unlike pairs is approximately twice the size of the smaller of the pair, but is still significantly greater than the size of the larger. We find that

β	L	Method	Sep.	$\langle R_{\min} \rangle$	$\langle \rho_{\text{eff}}(R_{\min}) \rangle$		# disc.	# used
2.4	16	$S(x)$	I-I	2.24(15)	2.93(06)	3.81(09)	48	213
			A-A	1.89(13)	2.90(06)	3.82(08)	51	210
			I-A	6.23(10)	3.20(06)	4.17(08)	46	215
			U/L	3.01(26)				
		$ Q(x) $	I-I	2.02(17)	2.98(05)	3.67(08)	56	205
			A-A	1.77(13)	2.95(05)	3.68(08)	57	204
			I-A	6.52(09)	3.18(06)	4.05(06)	59	202
			U/L	3.44(32)				
2.5	24	$ Q(x) $	I-I	1.62(16)	2.27(04)	2.84(07)	44	206
			A-A	1.25(11)	2.21(04)	2.83(06)	29	221
			I-A	5.92(11)	2.50(05)	3.15(06)	40	210
			U/L	4.14(47)				

Table 3: The average closest separation of *Like* pairs (I-I and A-A) and *Unlike* pairs (I-A). ‘Method’ indicates whether the sizes and locations were calculated using the action density $S(x)$ or the absolute topological charge density $|Q(x)|$. $\langle \rho_{\text{eff}}(R_{\min}) \rangle$ gives the average sizes of the closest objects, averaged over the ensemble of 250 configurations, with the left figure giving the average size of the smaller object. The last two columns indicate how many configurations were discounted from the calculations (for example a configuration with only one instanton was discounted from the I-I calculations) and how many from the ensemble were used. All sizes in units of ξ .

there is no appreciable difference in the ratio of size in like or unlike pairs, with the larger in the pair being 25–30% as big again as the smaller. Our lattice data is shown in table 3.

Recently [21] it has been proposed that the instantons and anti-instantons exist in isolated regions of the lattice, so that ‘bubbles’ of like objects exist. This could account for the observed behaviour in the closest separations shown in table 3. As a further probe of this we look at the distribution of separations, dN/VdR , for both like and unlike objects. Our results are given in figs. 8–10. The double peak structure of the like separation distribution is evidence that objects are localised within groups of like objects.

This is a striking result and we should consider whether it could be a consequence of our instanton finding algorithm. If an isolated instanton (or anti-instanton) were to have a sufficiently rough peak structure with several subsidiary peaks, then this would end up counted more than once. The consistency between the result obtained by analysing the $S(x)$ and the $|Q(x)|$ distributions does suggest that this is not an explanation of the enhanced signal of like species at small separation.

Defining a centre-of-mass x_c for the (anti-)instantons we looked at the proportion of objects located within certain radial distances of x_c . The results are shown in fig. 11. The shape of the curve, coupled with the data in figs. 8–10, implies that the (anti-)instantons are clustered in many small bubbles, as one large cluster would give a very sharp rise in the $P(R)$ curve and a single, broader peak in dN/VdR . Clearly this is an area in which further study is warranted.

7 Conclusions

Cooling is a local smoothing procedure which enables large scale excitations to be studied by reducing the quantum fluctuations. In order to obtain consistent results at different lattice spacings, it is essential to calibrate the cooling procedure. We explored this thoroughly in $O(3)$ where we used as a criterion the stability under cooling of an isolated instanton of a given physical size. In this work, we found that for $SU(2)$ (with the Wilson action), the isolated instanton configurations were extremely stable under cooling. Thus, as a calibration, we chose instead to create an isolated instanton solution, add the quantum fluctuations by simulation, and then select the cooling so that it removed these quantum fluctuations. Obviously, it would be possible to cool for some arbitrary amount, as in the majority of the literature, but we feel there should be some attempt made to justify the amount of cooling performed, and this calibration is essential if the cooling is performed, and the results compared, at different lattice spacings.

Our analysis shows that our resulting cooling prescription should preserve isolated instantons of size $\rho \geq a$. Of course, cooling could have a more pronounced effect in the realistic case of dense instantons: for instance by removing instanton–anti-instanton pairs which are close together or overlapping. This is hard to calibrate and must be remembered as a possible source of systematic error.

Compared to previous explorations of topological charge distributions in quenched $SU(2)$ and $SU(3)$ [3, 18], we have been able to study the topological charge distributions in our cooled configurations with large statistics, varying lattice spacing and large physical volume. We have made a comprehensive study of the size ρ of the peaks in the topological charge distribution. This size distribution increases as $\rho^{7/3}$ for a dilute instanton gas. We find a similar rapid increase for small ρ but then a maximum for $\rho \approx 0.3$ fm and a rapid decrease at larger ρ . Previous work [3] gave evidence for a peak in the size distribution on cooled configurations, whereas in citechu there is indication of a peak only in their more severely cooled data. We have explored this distribution in more detail and at different lattice spacings. The absence of important contributions from small objects agrees with earlier work. In particular, this explains why cooling gives a reasonable estimate [23] for the topological susceptibility - since the small objects which would be modified by cooling are not present anyway. Our conclusions are also compatible with phenomenological models for the QCD vacuum [22] which

require instantons of size $\rho \sim \frac{1}{3}\text{fm}$ with a density $n \sim 1\text{fm}^{-4}$.

Our results show some evidence that the peak in the size distribution is at smaller ρ for the smaller lattice spacing ($\beta = 2.5$). We also find a slight difference in the instanton density, namely $n(\beta = 2.4) = 0.71 \text{ fm}^{-4}$ and $n(\beta = 2.5) = 0.96 \text{ fm}^{-4}$. This residual dependence on β might be caused by our cooling calibration being not quite optimum and so corresponding to slightly stronger cooling at $\beta = 2.4$. Another possible explanation is that lattice artefacts in the instanton solution are important for $\rho < 2a$ and so are more significant at the larger lattice spacing. This uncertainty can be resolved by varying the cooling amount and by reducing the lattice spacing even further.

We have studied the relative disposition of instantons (I) and anti-instantons (A). We obtain the expected result that there is a minimum IA separation — since they will tend to annihilate if too close. We find, however, a surprising result: that there is a signal from II and AA pairs at close separation. This could arise if instantons were to exist in localised groups, well-separated from localised groups of anti-instantons. This clearly needs further work to establish the details of such a mechanism.

Acknowledgements

We are indebted to Claus Montonen for bringing our attention to references [5] and [6]. This research was carried out as part of the EC Programme “Human Capital and Mobility” — project number ERB-CHRX-CT92-0051.

Figures

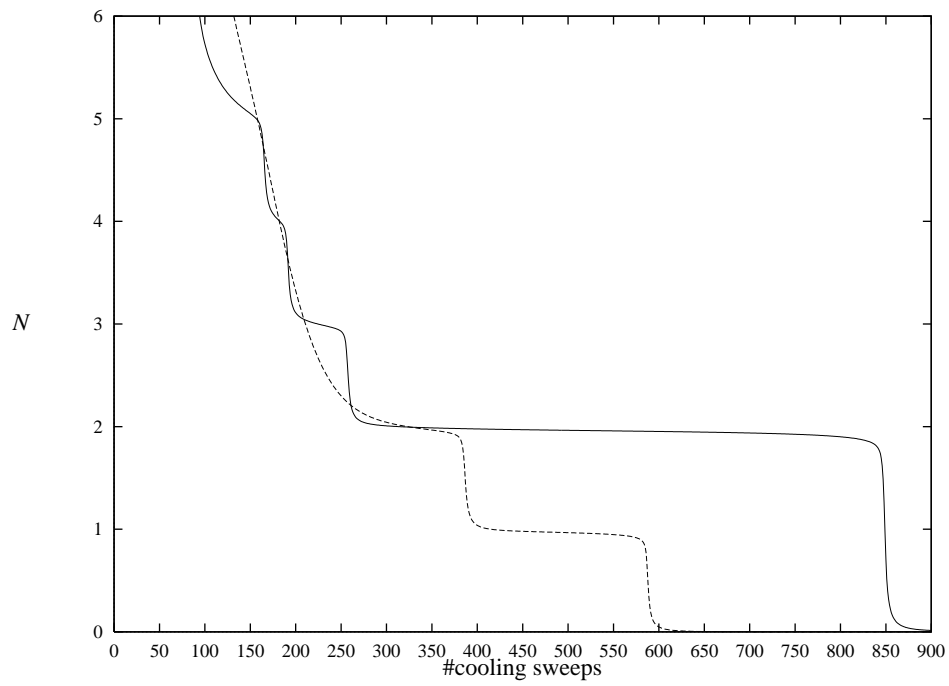


Figure 1: $N (S/S_I)$ for two example $SU(2)$ configurations as they are cooled with $\alpha = 2$.

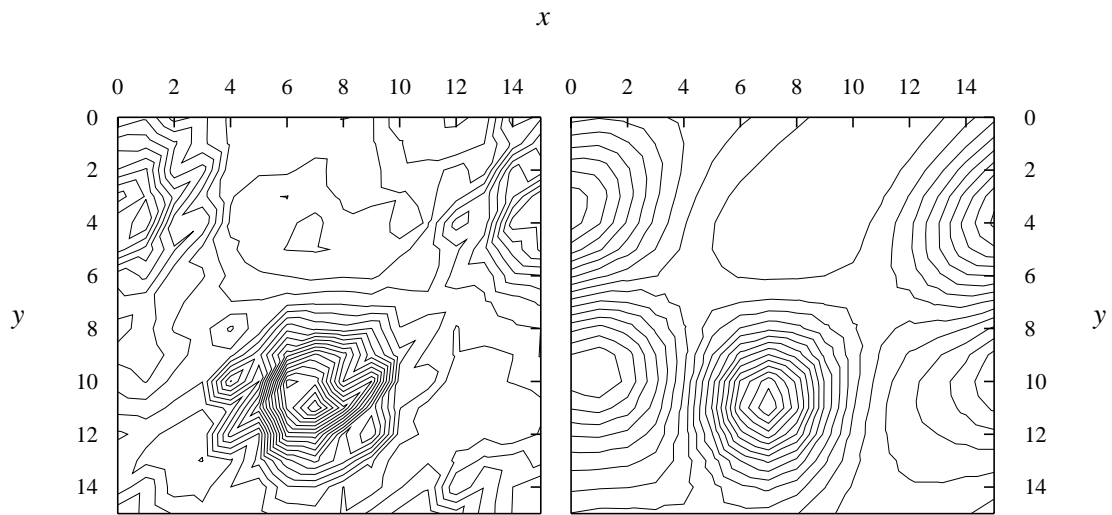


Figure 2: Contour plots for fig. 3. $S(x, y, 14, 9)$ is the left plot and $Q(x, y, 14, 9)$ is the right plot.

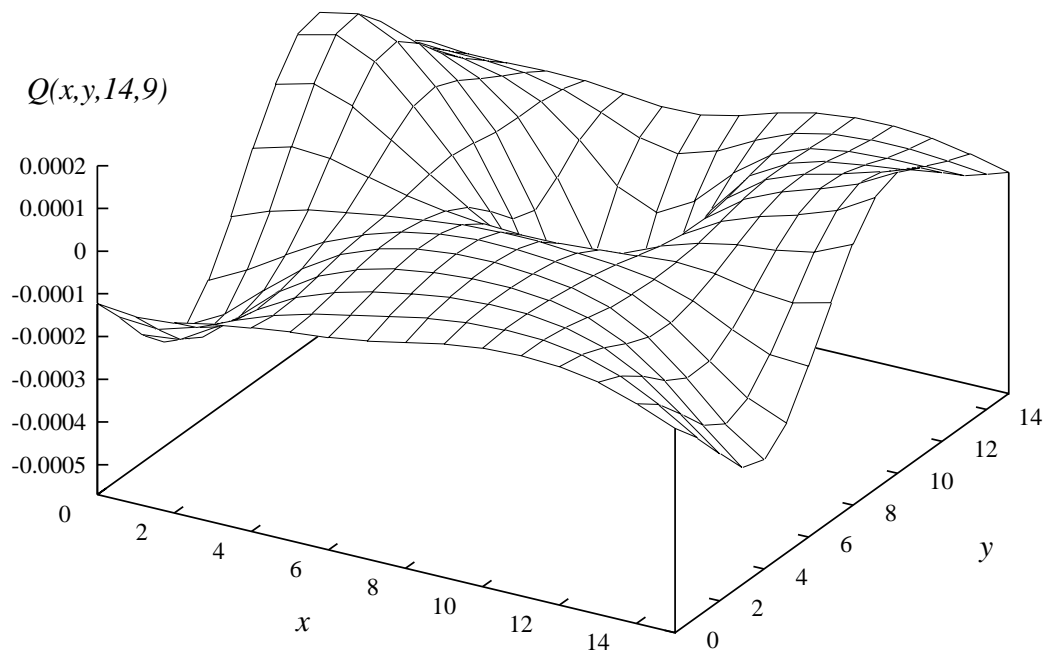
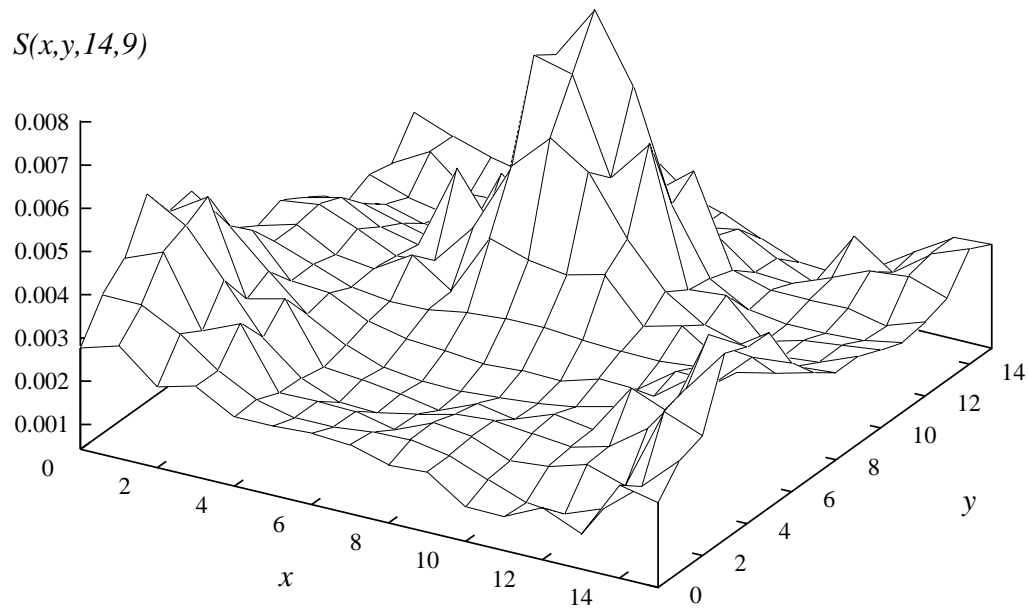


Figure 3: The action and topological charge densities for the $(x, y, 14, 9)$ plane from a sample configuration, generated at $\beta = 2.4$ on a 16^4 lattice.

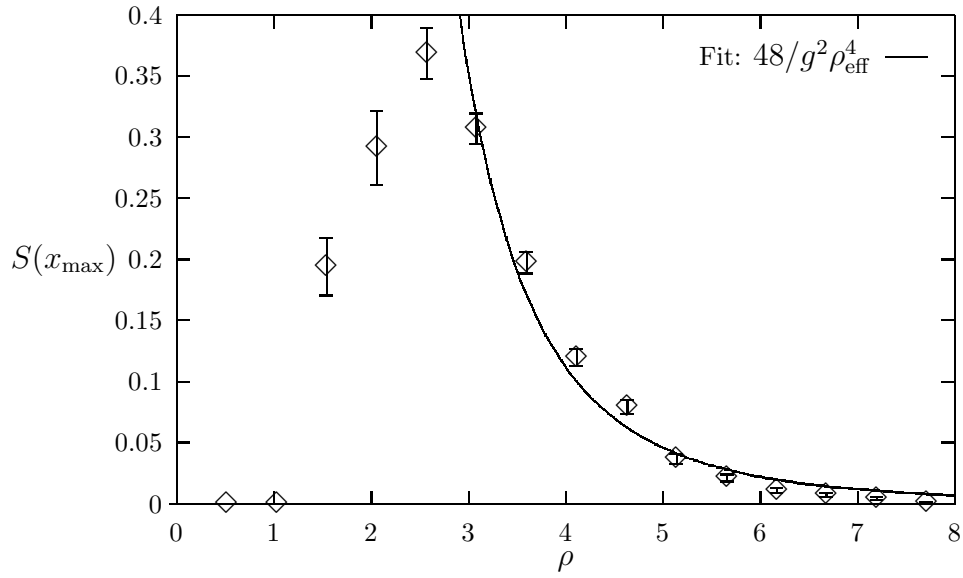


Figure 4: Peak height against instanton size ρ (in units of the glueball mass) calculated using $S(x)$ on a 16^4 lattice at $\beta = 2.4$.

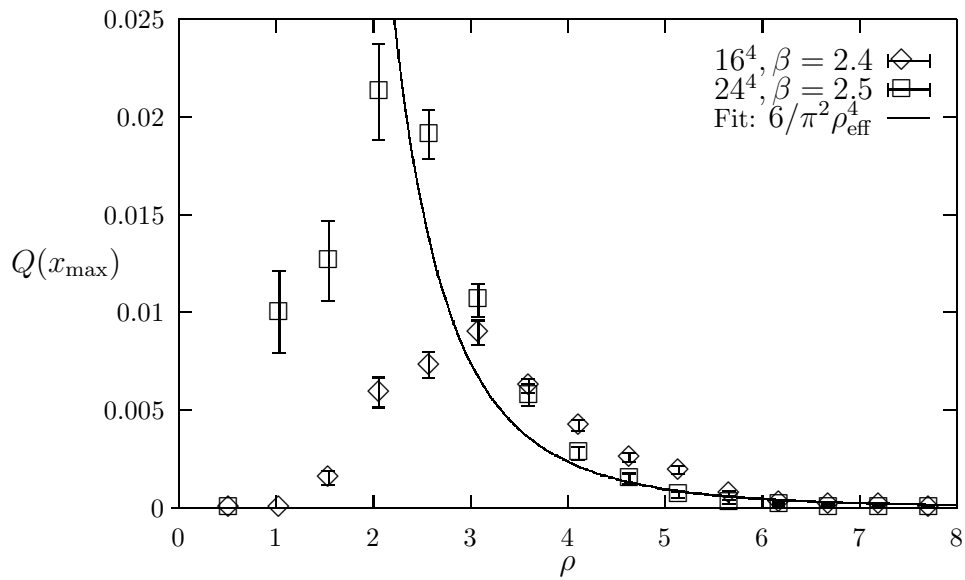


Figure 5: Peak height against instanton size ρ (in units of the glueball mass) calculated using $|Q(x)|$.

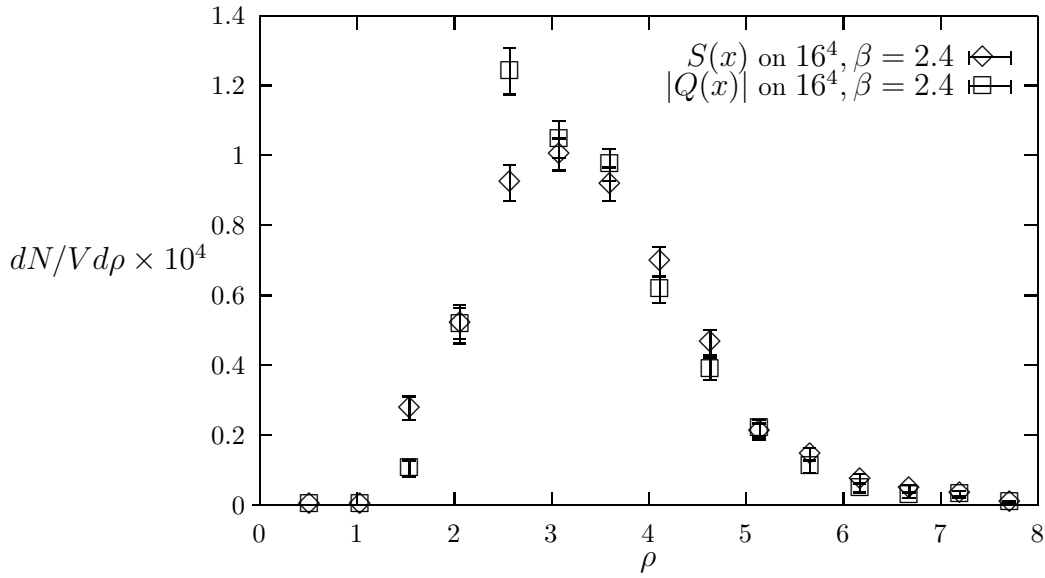


Figure 6: Size distributions (ρ in units of the glueball mass) calculated on a 16^4 lattice at $\beta = 2.4$.

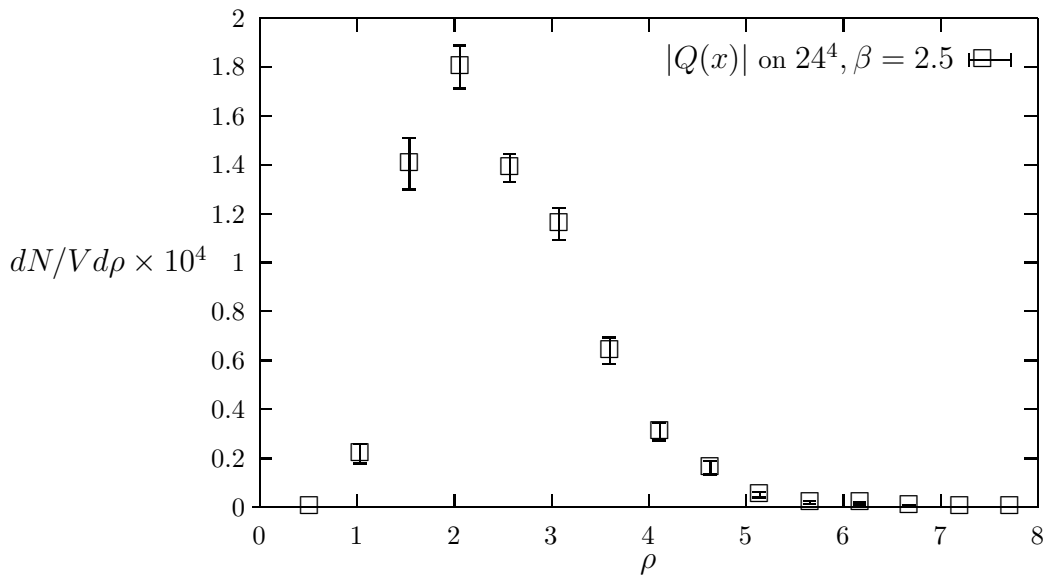


Figure 7: Size distributions (ρ in units of the glueball mass) calculated on a 24^4 lattice at $\beta = 2.5$.

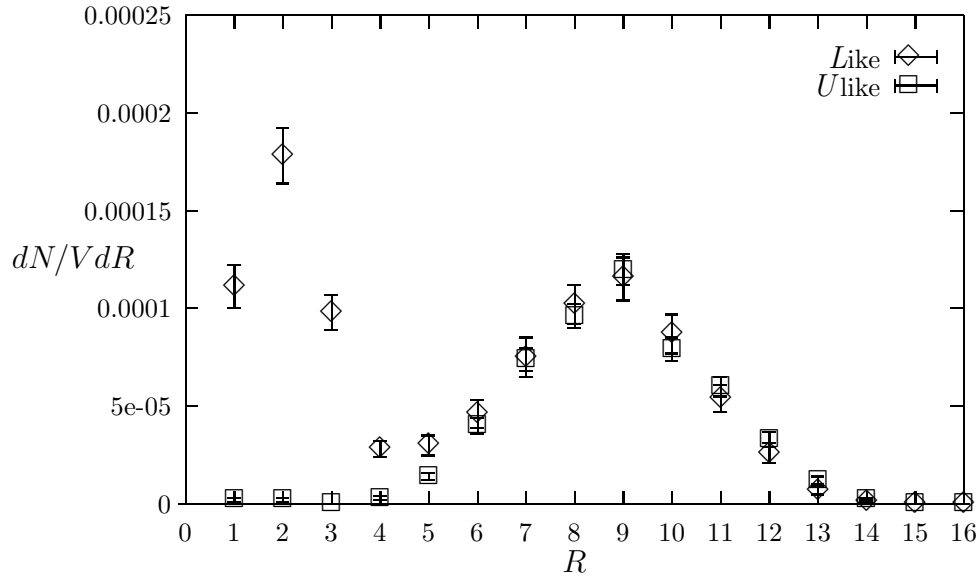


Figure 8: The data for the distribution of separations of like and unlike pairs (in units of the glueball mass), calculated at $\beta = 2.4$ on a 16^4 lattice using $S(x)$.

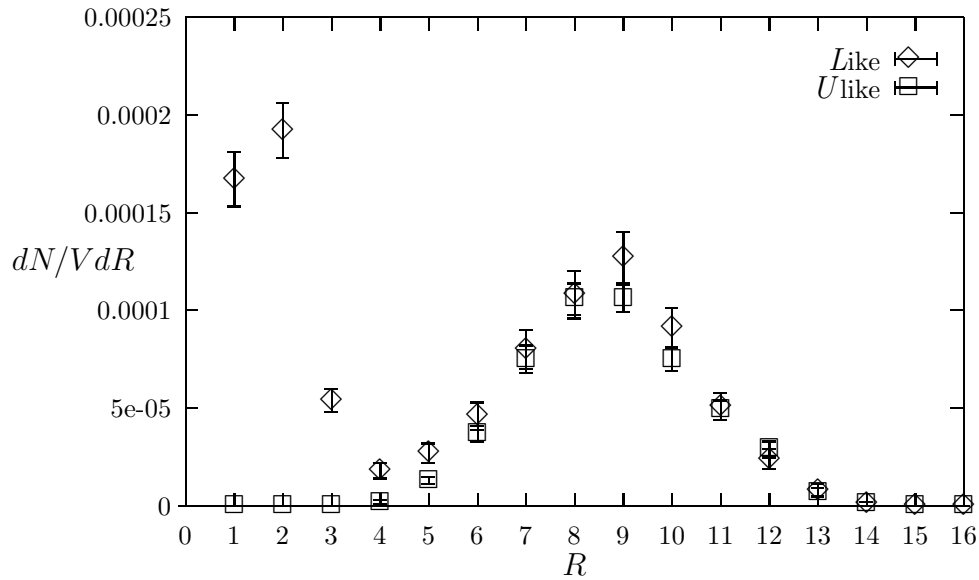


Figure 9: The data for the distribution of separations of like and unlike pairs (in units of the glueball mass), calculated at $\beta = 2.4$ on a 16^4 lattice using $|Q(x)|$.

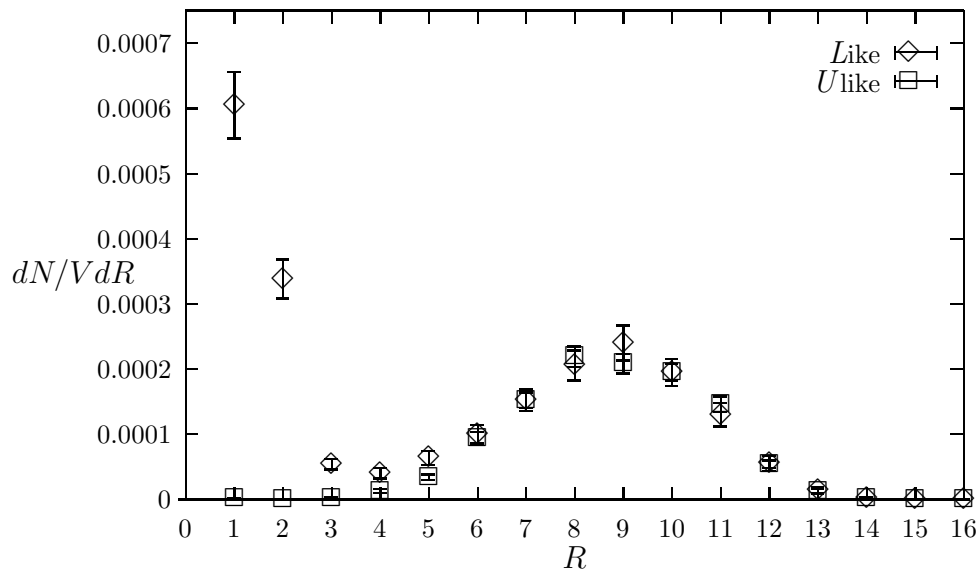


Figure 10: The data for the distribution of separations of like and unlike pairs (in units of the glueball mass), calculated at $\beta = 2.5$ on a 24^4 lattice using $|Q(x)|$.

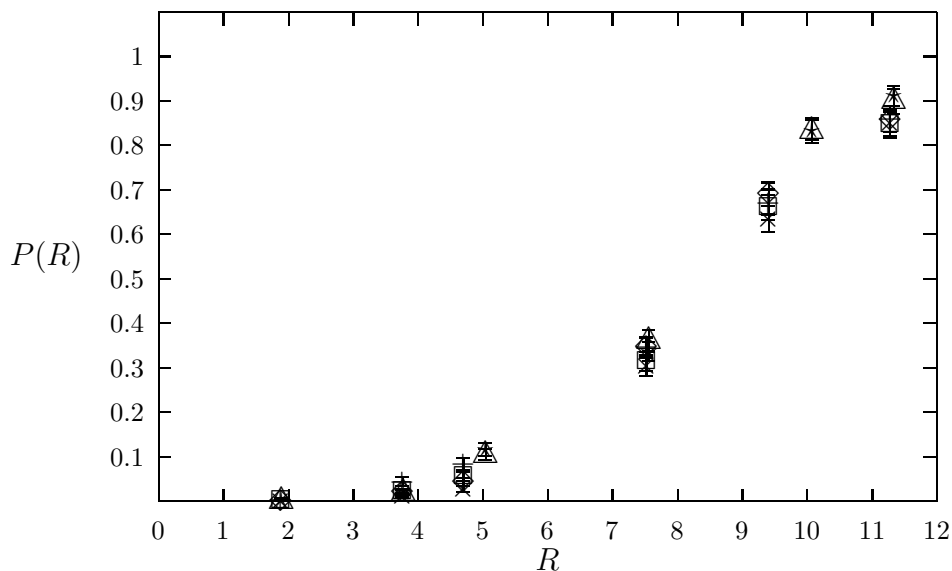


Figure 11: The proportion, $P(R)$, of objects found within a distance R (in units of the glueball mass) of the centre-of-mass calculated as follows: at $\beta = 2.4, 16^4$ using $S(x)$, I (\diamond), A ($+$), using $|Q(x)|$, I (\square), A (\times); and at $\beta = 2.5, 24^4$ using $|Q(x)|$, I (\triangle), A (\star).

References

- [1] M. Teper, Phys. Lett. **162B**, 357 (1985).
- [2] E.-M. Ilgenfritz, M.L. Laursen, M. Müller-Preussker, G. Schierholz, H. Schiller, Nucl. Phys. **B268**, 693 (1986).
- [3] M.I. Polikarpov, A.I. Veselov, Nucl. Phys. **B297**, 34 (1988).
- [4] A.A. Belavin, A.M. Polyakov, A.S. Schwatz and Yu.S. Tyupkin, Phys. Lett. **59B**, 85 (1975).
- [5] D. Förster, Phys. Lett. **66B**, 279 (1977).
- [6] W. Palmer & S.S. Pinsky, Phys. Rev. **D21**, 551 (1980).
- [7] *Instanton size distributions from calibrated cooling*, C. Michael & P.S. Spencer, Liverpool Preprint LTH-337, Helsinki preprint HU-TFT-94-45, to appear in the proceedings of LATTICE'94.
- [8] *Gauge theory of elementary particle physics*, Ta-Pei Cheng and Ling-Fong Li, Oxford University Press (1984).
- [9] M.L. Laursen, J. Smit, J.C. Vink, Nucl. Phys. **B343**, 522 (1990).
- [10] *Topography of the cooled $O(3)$ vacuum*, P.S. Spencer and C. Michael, Liverpool preprint LTH 328, hep-lat/9401011, submitted to J. Phys. G.
- [11] C. Michael & P.S. Spencer, Phys. Rev. **D50**, 7570 (1994).
- [12] *Large Instantons In Lattice Gauge Theory And Their Stability Under "Cooling"*, M. Teper, Oxford University preprint 59/88
- [13] A.M. Green, C. Michael, J.E. Paton, M.E. Sainio, Int. J. Mod. Phys. **E2**, 479 (1993).
- [14] J. Fingberg, U.M. Heller, F. Karsch Nucl. Phys. **B392**, 493 (1993).
- [15] M. Campostrini *et al*, Nucl. Phys. **B329**, 683 (1990).
- [16] *Topological density and instantons on a lattice*, J. Grandy & R. Gupta, contribution to LATTICE '94.
- [17] C. Michael, G.A. Tickle, M. Teper Phys. Lett. **207B**, 313 (1988).
- [18] M.-C. Chu, J.M. Grandy, S. Huang, J.W. Negele, Nucl. Phys. B (Proc. Suppl.) **34**, 170, (1994);
M.-C. Chu, J.M. Grandy, S. Huang, J.W. Negele, Phys. Rev. **D49**, 6039 (1994).

- [19] *Peeping into the $SU(2)$ gauge vacuum*, A. Gonzales-Arroyo, FTUAM-94-26, hep-lat/9502014, contribution to LATTICE '94.
- [20] This relation occurs in many papers and textbooks. Amongst others:
Gauge fields and strings A.M. Polyakov, North Holland (1982);
The uses of instantons, S. Coleman, in *The Whys of Subnuclear Physics*, ed. A. Zichichi, Plenum Press, New York (1979);
Solitons and instantons, R. Rajaraman, North Holland (1982).
- [21] A. Gonzales-Arroyo, talk given at Cortona.
- [22] E. Shuryak, *Rev. Mod. Phys.* **65**, 1 (1993).
- [23] B. Alles *et al*, *Phys. Rev.* **D48**, 2284 (1993).